Carbohydrate Polymers 90 (2012) 1353–1361

Contents lists available at SciVerse ScienceDirect

Carbohydrate Polymers

journal homepage: www.elsevier.com/locate/carbpol

Preparation, characterization and cytocompatibility of polyurethane/cellulose based liquid crystal composite membranes

Wanqing Han[a,b], Mei Tu[a,b,*], Rong Zeng[a,b], Jianhao Zhao[a,b], Changren Zhou[a,b]

[a] Department of Materials Science and Engineering, College of Science and Engineering, Jinan University, Guangzhou 510632, PR China
[b] Engineering Research Center of Artificial Organs and Materials, Ministry of Education, Guangzhou 510632, PR China

ARTICLE INFO

Article history:
Received 16 April 2012
Received in revised form 24 June 2012
Accepted 2 July 2012
Available online 9 July 2012

Keywords:
Polyurethane
Liquid crystal
Composite membrane
Surface aggregate structure
Cell compatibility

ABSTRACT

Two types of polyurethane/liquid crystal (PU/LC) composite membranes with different LC contents, namely polyurethane/octyl hydroxypropyl cellulose ester (PU/OPC) and polyurethane/propyl hydroxypropyl cellulose ester (PU/PPC), were prepared and studied. The effects of surface properties on cell compatibility of the membranes were elucidated. PPC tended to assemble to independent phases in the composite membranes, while OPC formed uniformly distributed LC domains. As the introduction of LC, phase separation occurred, and the crystallization of PU was disrupted. The surface of PU/LC composite membranes showed fingerprint texture and two-phase morphology. Hydrophilicity of the two types of composite membranes exhibited a reversal tendency with the increase of LC contents. Cells seeded on the composite membranes presented favorable growth when the content of LC was over 30%, especially on PU/OPC complex. The surface morphology, phase separation between LC and PU as well as the type of LC showed significant effects on the cell behaviors.

1. Introduction

The biocompatibility of material is determined by the information transfer among the material, interfacial protein, cell and biological system (De Oca et al., 2010; Fong, Hanley, & Boyd, 2009; Lutolf, Gilbert, & Blau, 2009), in which, the surface of biomaterial plays a key role in controlling cellular behaviors (Ranella, Barberoglou, Bakogianni, Fotakis, & Stratakis, 2010). Cell behaviors can be regulated by the surface roughness and hydrophilicity of materials, as well as the specific interaction between cells and material surfaces. Much research has revealed that the interactions between cells and matrix were meditated by the 'bio-recognition processes' (Kasemo, 2002), such that novel bio-functionalized surfaces are required to possess biorecognition ability to biological systems (Ma, Mao, & Gao, 2007). Some strategies in surface engineering of biomaterials by biomimetic process have been developed. Specifically, those combinations of topographic, chemical composition and viscoelastic patterns on surfaces to affect the cellular responses and produce 'contact guidance' (Bruckmann, Walboomers, Matsuzaka, & Jansen, 2005; Singhvi, Stephanopoulos, & Wang, 1994) were highly appreciated. Among all kinds of engineered materials, biomimetic materials have attracted the most concerns for their abilities of creating an excellent artificial extracellular matrix (ECM) to induce specific physiological response of cells.

Liquid crystals (LC) have been widely used in dynamically functional materials, including electro-optical displays and sensors (Hwang et al., 2002), owing to their changeable molecular arrangements in different external environments, such as magnetic field, electric field and temperature (Ignés-mullol & Schwartz, 2001; Kaneko, Yamaoka, Osada, & Gong, 2004; Matsusaki, Thi, Kaneko, & Akashi, 2005). Recently, LC science has been attracted more interest in a new field – bioscience that mimics the biological environment and system (Stewart, 2003, 2004). Actually, liquid crystalline morphology can been found in many biological systems (Aouada, De Moura, Fernandes, Rubira, & Muniz, 2005; Woltman, Jay, & Crawford, 2007). For example, cell membranes, proteins, phospholipids, cholesterols and DNA are also known to exist as LC phase (Bouligand & Norris, 2001; Caffrey, 2003; Smeller, 2002) that is an active substrate for cell–matrix interaction. In addition, liquid crystalline polymers with ordered arrangement, showing a soft elasticity (Rey, 2005) and self-organized structure through non-covalent specific interactions with living system, would be useful in bio-related fields (Bruckmann et al., 2005; Hwang et al., 2002; Kaneko et al., 2004; Lockwood et al., 2006; Ma et al., 2007; Singhvi et al., 1994). Nagahama, Ueda, Ouchi, and Ohya (2007) have

Abbreviations: OPC, octyl hydroxypropyl cellulose ester; PPC, propyl hydroxypropyl cellulose ester; LC, liquid crystal.

* Corresponding author at: Department of Material Science and Engineering, College of Science and Engineering, Jinan University, Huangpu Road 601, Guangzhou 510632, PR China. Tel.: +86 20 85223271; fax: +86 20 85223271.
E-mail address: tumei@jnu.edu.cn (M. Tu).

0144-8617/$ – see front matter © 2012 Elsevier Ltd. All rights reserved.
http://dx.doi.org/10.1016/j.carbpol.2012.07.004

prepared biodegradable liquid crystalline materials with cholesterol side-functionalized poly(depsipeptide-co-DL-lactide) that served as physical cross-linking points to form non-covalent network in the polymer matrix. This kind of liquid crystalline material may be a new candidate of implantable biomaterials for dynamic organs like heart and blood vessels. Hwang et al. (2002) have also found cholesteryl-(L-lactic acid) scaffold with consistent spatial orientation could promote initial cell adhesion and sustained delivery of vital biological molecules. In our previous work, we have prepared a series of composite membranes of polymer/cholesteryl tetraethylene glycol carbonate (CTgC) for improving the blood compatibility of composite materials and found that CTgC phase would be separated from the polymer substrate and mainly distributed on the membrane surfaces, which was mimicking the structure of LC state of vascular intima and therefore showed excellent hemocompatibility (Li, Tu, Mou, & Zhou, 2001; Zhou & Yi, 1999). The size and distribution of LC domains, phase separation between polymer and LC regions, as well as the LC content could influence the surface properties of the composite membranes so as to affect the protein adsorption on the membrane surface and the biocompatibility. However, the low molecular weight CTgC was likely to escape from the composite membranes because of its weakly interaction with the polymer matrix (Xie, 2007). For that, LC compounds of hydroxypropyl cellulose derivatives with a high molecular weight have been attempted for polymer/LC composite materials.

In this study, two types of PU/LC composite membranes with different LC contents by blending hydroxypropyl cellulose derivative LC with polyurethane (PU) were fabricated via a film forming technique. The phase separation behavior, surface morphology, crystallization and wettability of membranes were characterized by polarized optical microcopy (POM), scanning electron microcopy (SEM), X-ray diffraction (XRD) and static contact angle respectively. Additionally, cell compatibility tests were performed to investigate the interaction between cells and PU/LC composite membrane surfaces.

2. Materials and methods

2.1. Materials

PU [$M_w = 2.7 \times 10^5$, containing 35 wt% hard segment 4,4@-methylene diphenylene diisocyanate and 65 wt% soft segment polyether], medical grade, was purchased from Yin Tesheng Co. of Guangzhou, China. All other reagents and solvents used were analytical grade. Octyl hydroxypropyl cellulose ester (OPC, $M_w = 9.37 \times 10^4$) and propyl hydroxypropyl cellulose ester (PPC, $M_w = 9.31 \times 10^4$) with the thermal transition temperature of $T_{g(OPC)} = 16.5\,^\circ C$, $T_{NI(OPC)} = 132.5\,^\circ C$; $T_{g(PPC)} = 34.9\,^\circ C$, $T_{NI(PPC)} = 155.6\,^\circ C$ were esterified from hydroxypropyl cellulose ($M_w = 10$ W, Sigma, USA) in our lab (Gong, 2011). The chemical structure of LC compound was shown in Fig. 1.

2.2. Preparation of PU/LC composite membranes

A series of built-up PU/LC composite membranes were prepared via a solution-casting method. After dissolving the PU and LC into tetrahydrofuran at room temperature, clear and homogeneous mixture was obtained with the weight ratio of the PU:LC at 9:1, 7:3 and 5:5, defined as PU/LC-10, PU/LC-30 and PU/LC-50 respectively, where the LC referred to OPC or PPC. The solution was cast onto clean glass plate and then the solvent was evaporated for 72 h at room temperature, membranes were further dried in vacuum at 25 °C for 10 h to eliminate the residual solvent. The thickness of the composite membranes and aggregation state of LC in the composite membranes could be controlled by altering the solvent, the concentration of solution or the evaporation speed of solvent. Series of membranes including pure PU, PU/LC-10, PU/LC-30, PU/LC-50, and pure LC were prepared for characterization.

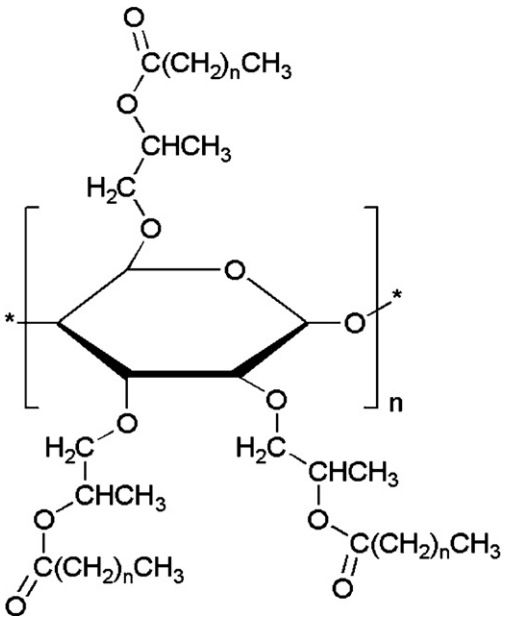

Fig. 1. Chemical structure of LC compound, $n = 1$ for PPC and $n = 6$ for OPC.

2.3. Surface texture

2.3.1. Polarized optical microscopy (POM)

POM (Olympus BX51, Germany) was utilized to view the texture of optical anisotropic PU/LC composites. The microscope used in this work was equipped with a polarizer at the base and an analyzer at 90° above the objective lens. The samples were attached to grass slip between the two polarizers, and images were recorded by using Linksys 2.43 Software at 25 °C.

2.3.2. Scanning electron microscopy (SEM)

Scanning electron microscopy (PHILIPSXL-30ESEM) was used to observe the surface topography of tested membranes. All specimens were spattered a gold layer in a sputter coater (BAL-TEC, SCD005), and then surface morphological observation was performed.

2.4. X-ray diffraction (XRD)

The crystallization of the membranes was measured with a Dmax-1200 diffractometer (Japan) using Cu Kα radiation generated with 30 kV and 20 mA. The solution-casting specimens were placed vertically (flow direction in the vertical) and perpendicularly to the incident X-ray beam. The experimental set-up allowed for the simultaneous acquisition of wide-angle bidimensional scattering patterns. Five films were stacked in aluminum holders and scanned at room temperature over the 2θ range 5–40° with scanning rate of 8°/min. Data were recorded at the interval of 0.02°.

2.5. Mechanical properties

The tensile properties of the PU/LC composite membranes with various LC contents (1 cm in width, 10 cm in length, and 200 μm in height) were measured on a universal material testing machine (BT1-FB005TN.D14, Zwick, Germany) at a crosshead speed of 20 mm/min. The initial linear modulus on the stress–strain curve was defined as the elastic modulus of the membrane. The reported

values were calculated as averages over five specimens for each composition.

2.6. The static contact angles

The measurement of the static water contact angle was performed for evaluation of surface wettability of composite membrane. Drop Shape Analysis System DSA100 (Krüss, Germany) was used to measure the static contact angles of the air side of all samples against water at room temperature. The average value was calculated based on measurements at 10 different positions in each sample eliminating the maximum and minimum.

2.7. Cell compatibility study

2.7.1. Fibroblast cell culture

Mouse embryonic fibroblasts 3T3 (provided by Laboratory of Biomedical Engineering, Jinan University) were used for the cell experiments. Cells were cultured in L-DMEM medium supplemented with 10% fetal bovine serum (FBS, Gibco, BRL) and 1% penicillin/streptomycin (Gibco, BRL) at 37 °C in a 5% CO_2 supplied incubator. Culture medium was refreshed every two days.

2.7.2. Cell viability test

All tested membranes were transferred to 24-well plates after 2 h UV radiation for each side. Cells were harvested at the confluent of 75% in a 0.025% trypsin/EDTA and seeded at a density of 10^5 cells/cm^2. The activity of cultured cells was measured with MTT colorimetric assays (Vihola, Laukkanen, Valtola, Tenhu, & Hirvonen, 2005). At the designed period of 1, 3, 5 and 7 days, cells were incubated for a further 4 h at 37 °C after adding 20 μL 5 mg/mL MTT solution. The MTT was reduced to an insoluble formazan precipitate by mitochondrial succinic dehydrogenase of viable cells. The solution was removed and 1 mL of lysis solution was added to each well to stop the reaction. After another 4 h incubation with complete dissolution of the dark-blue crystal of MTT formazan, 200 μL of the clear solution was transferred to a 96-well culture plate, and the absorbance of the content of each well was measured at a wavelength of 490 nm with a microplate reader on a spectrophotometer against a blank of lysis solution.

2.7.3. Initial cell adhesion and morphology observation

Cell initial adhesion and morphology observation was performed by SEM. To co-culture of fibroblasts with sterilized membranes, the same procedures were performed as that of cell viability test. At the cultivation periods of 2 h and 3 days, the samples were rinsed gently with phosphate buffer solution (PBS) for 3× 10 min and fixed with 2.5% glutaraldehyde in PBS for 30 min at 4 °C. After dehydration in graded alcohols, samples were mounted on copper stubs, coated with gold and examined by SEM with an acceleration voltage of 20 kV.

3. Results and discussion

3.1. Optical texture and surface morphology

Fig. 2 shows the optical texture images of all membranes. The pure PU film presented smooth surface and dark view under cross polarization (Fig. 2a). After blending with LC compounds, well-dispersed birefringence occurred at all PU/LC composite membranes (Fig. 2b–g), exhibiting bright spots for the formation of LC domains. The size and number of LC domains increased with the LC content. The LC domains distributed uniformly over the PU/OPC composite membranes with dots shape (Fig. 2b–d), while those among the PU/PPC formed stripe-like veins at a low LC content of less than 30% (Fig. 2e and f), but aggregated into disk texture when increasing the LC content to over 30% (Fig. 2g). These results indicated that after incorporating LC into PU substrate, phase separation took place in the composite membranes due to the partially immiscibility of these two components. As shown in Fig. 1, the chemical structure of LC consists of cyclic rings and flexible side-chains. However, PPC possessed shorter soft side-chains so that exhibited stiffer macromolecular backbone due to the stronger interaction among main chains. Hence, PPC tended to aggregate to form independent phases in the composite membranes, which resulted in the formation of larger LC domains as observed in the field of POM (Fig. 2e and f). By contrast, OPC presented semi-rigid chain structure for its longer flexible side-chains; meanwhile those longer side-chains could entangle with the soft segments of PU chains, which was in favor of the uniform distribution of LC domains in composites (Fig. 2b–d).

The surface morphologies of all membranes were observed by SEM (Fig. 3). The pure PU film considerably exhibited a flat surface without any textures (Fig. 3a), while both pure LC films and all PU/LC composite membranes displayed coarse and a two-phase morphology. The interlaced network texture appeared on the surface of these two pure LC films is highly similar to the characteristic oily streaks of cholesteric liquid crystal (Lin, Huang, & Chen, 2011). With regard to the PU/LC composite membranes, the LC domains showed scattered fingerprint texture dispersing on the membrane surface at a low LC content (Fig. 3b and f), representing a small number of LC organized to ordered phases. With the increase of LC content, the 'fingerprint' configuration grew bigger and denser gradually (Fig. 3c, d, g, h), and connected with each other as well. These two types of PU/LC composite membranes showed little difference in the surface morphology.

3.2. XRD analysis of PU/LC composite membranes

XRD patterns of all kinds of membranes were presented in Fig. 4. For PU films, because of the ordered arrangement of soft segments (Kovacevic et al., 1990, 1993), the diffraction peaks at 2θ of 10° and 20° were the characteristic peaks of semi-crystallization of PU. Meanwhile, two broad and flat diffraction peaks also emerged at nearly the same positions for the two types of pure LC membranes, which might be attributed to the short range or quasi-long-range positional order of the LC macro-molecular chains (Bettini, Romani, Morganti, & Borghetti, 2008). For PU/LC composite membranes, the corresponding peaks became broader with lower intensities by increasing the LC content. It suggested that the introduction of LC into PU substrate might change its initial crystalline behavior. Interestingly, the diffraction peak at the 2θ of 20° almost disappeared for PU/OPC composite membrane with a LC content of 50%. It was possible that in the complex system of PU and LC, the hydrogen bonds between hard and soft segments and among hard ones within PU were partially broken at the presence of LC compounds, and therefore affected the crystallization of PU. In contrast, PPC possessed higher potential to aggregate into isolate phase during the films formation, which had no significant influence on the crystalline behavior of PU. So the two diffraction peaks of PU/PPC composite membranes just broaden gradually with the decrease of PU content. Nevertheless, the flexible OPC chains might entangle with the soft segments of PU through their longer soft side-chains, which more interrupted the crystallization of PU. Especially when the OPC approached to 50%, it assembled dramatically and formed continuous LC phases throughout the substrate. Such that, the crystalline structure of PU was destroyed heavily and the diffraction peak at the 2θ of 20° disappeared.

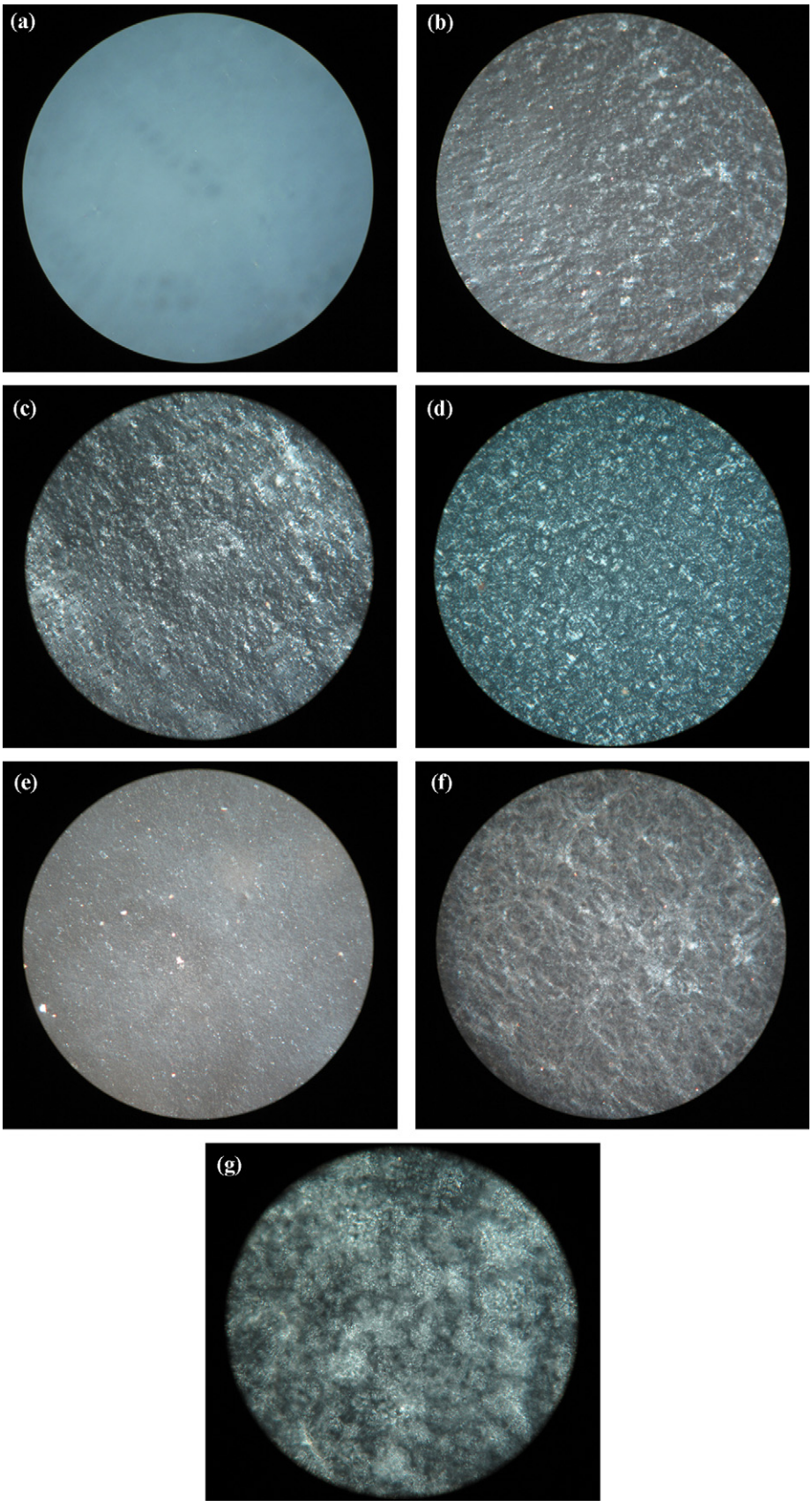

Fig. 2. POM images of two types of PU/LC composite membranes (500×). (a) Pure PU film; (b–d) PU/OPC composite membranes with OPC content of 10%, 30% and 50% respectively; (e–g) PU/PPC composite membranes with PPC content of 10%, 30% and 50% respectively.

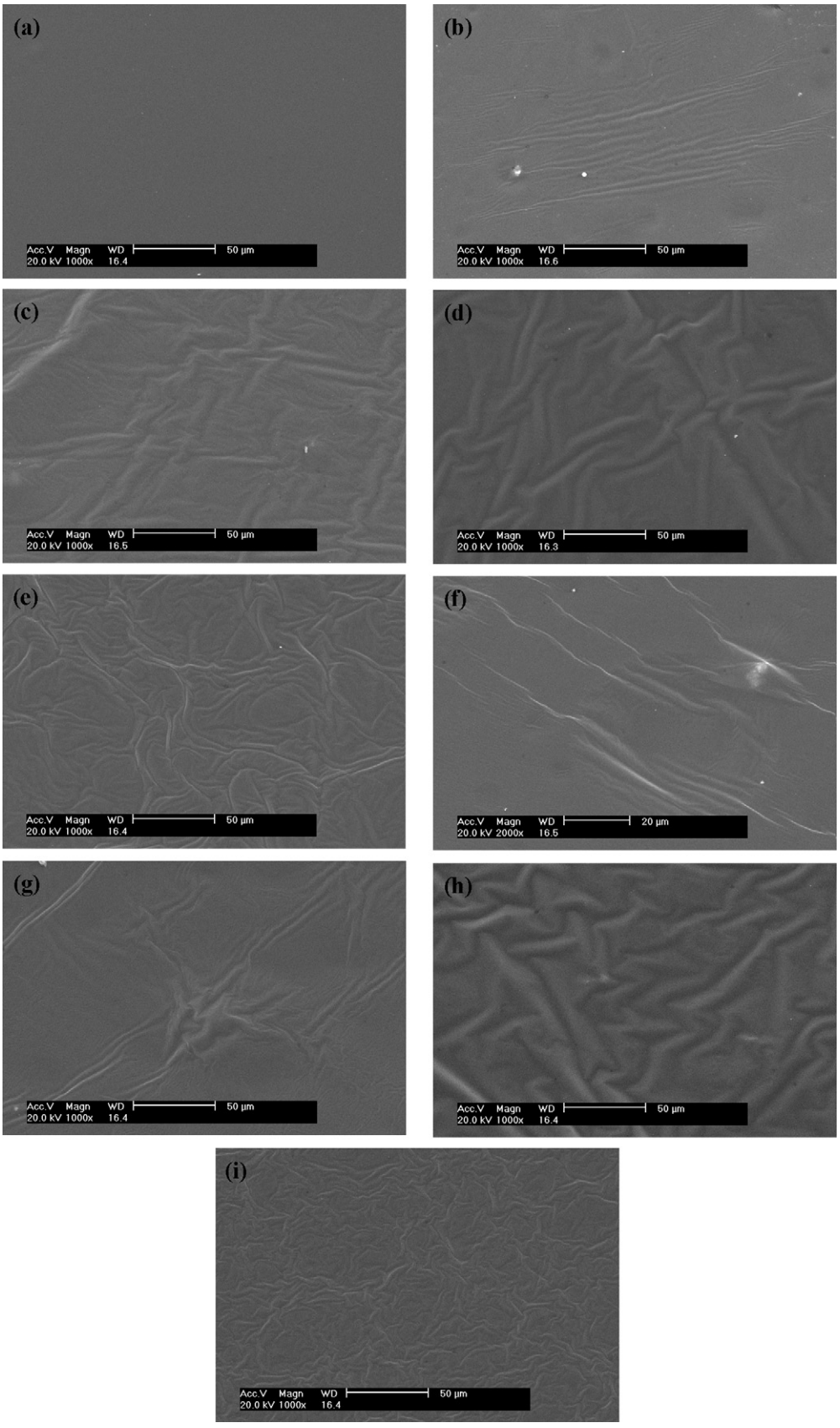

Fig. 3. SEM micrographs of PU/LC composite membranes. (a) Pure PU film; (b–e) PU/OPC composite membranes with OPC content of 10%, 30%, 50% and 100% respectively; (f–i) PU/PPC composite membranes with PPC content of 10%, 30%, 50% and 100% respectively.

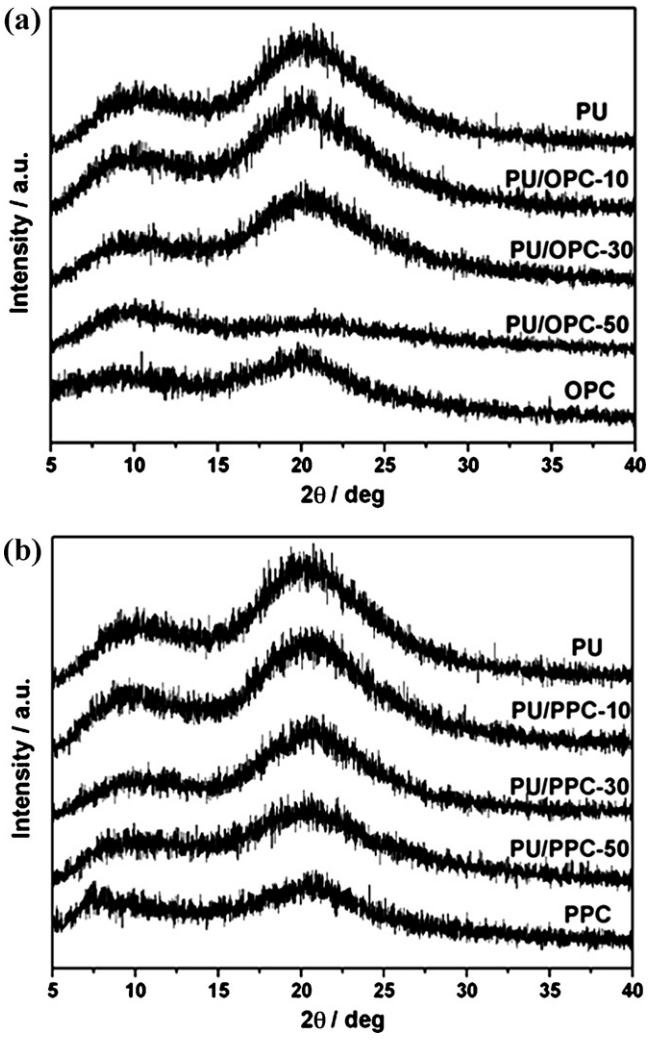

Fig. 4. XRD profiles of PU/LC composite membranes. (a) PU/OPC composite membranes and (b) PU/PPC composite membranes.

3.3. Elastic modulus

The elastic moduli of various membranes were shown in Fig. 5a. The initial tensile modulus of pure PU membrane was 13.3 ± 0.8 MPa, and decreased with the increase of LC content.

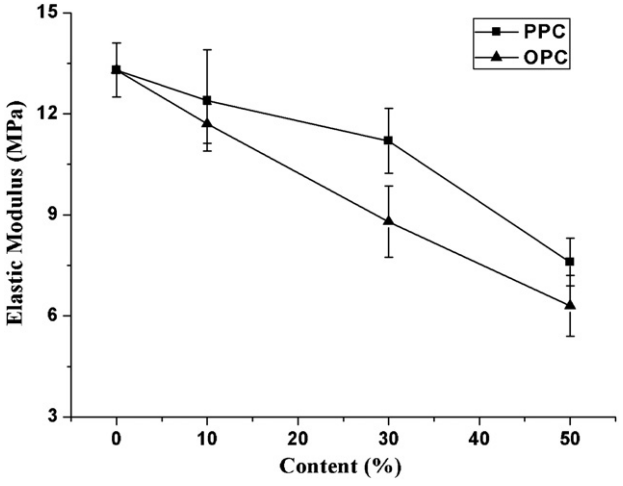

Fig. 5. Elastic moduli of the various PU/LC composite membranes.

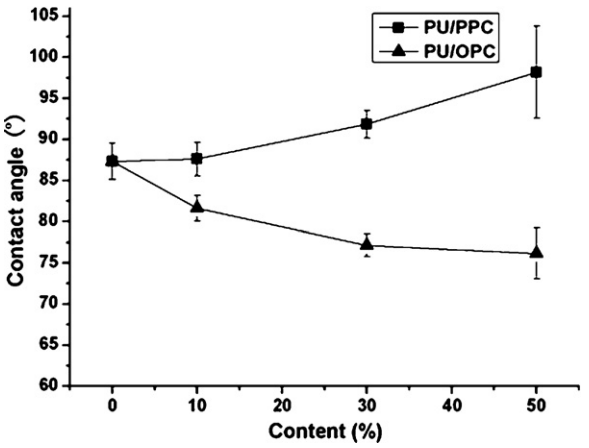

Fig. 6. Static water contact angles of PU/LC composite membranes with different LC contents.

Compared to PU/PPC, the PU/OPC composite membrane at the same LC content presented a lower elastic modulus, which may be attributed to the longer flexible side-chain of the OPC that led to the softer LC phase in the composite. Though the introduction of LC would decreased the modulus of the matrix, the PU/LC composite still remained a relatively high mechanical property.

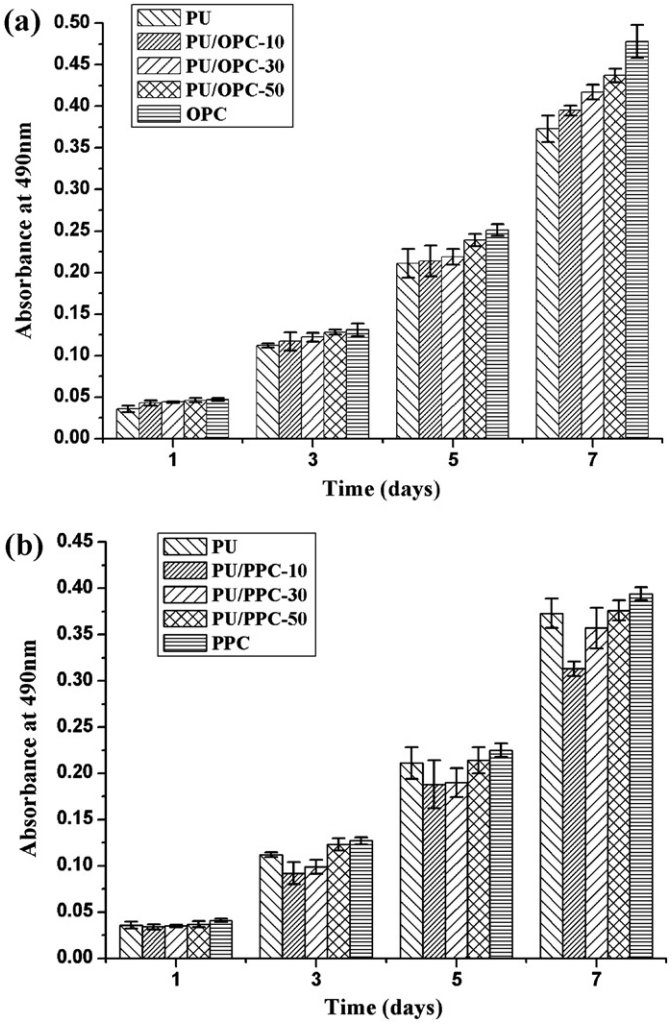

Fig. 7. MTT assays of 3T3 fibroblasts on different surfaces during the observation periods. (a) PU/OPC composite membranes and (b) PU/PPC composite membranes.

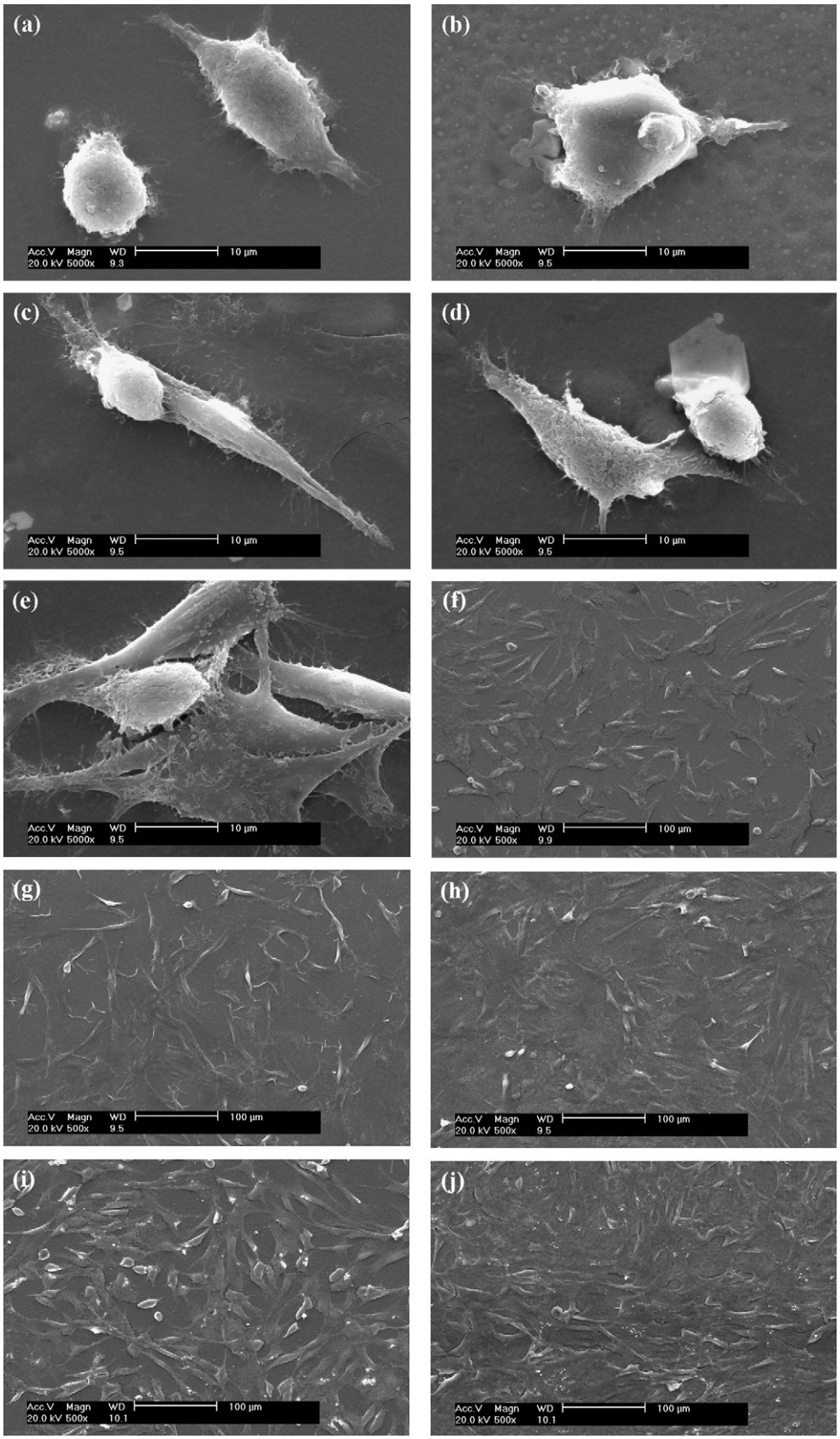

Fig. 8. SEM micrographs of 3T3 fibroblasts seeded on the tested membranes. (a–e) 2 h cultivation on PU/OPC composite membrane with OPC content of 0%, 10%, 30%, 50% and 100% respectively; (f–j) 3 days cultivation on PU/OPC composite membrane with OPC content of 0%, 10%, 30%, 50% and 100% respectively.

3.4. Water contact angles of PU/LC composite membranes

Static water contact angles were measured to evaluate the wettability of all membranes (Fig. 6). The tendency of water contact angles changing with the LC contents was totally different for the two types of PU/LC composite membranes. With the increase of LC from 0% to 50%, the water contact angles of PU/OPC decreased from 87° to 76°, while that of PU/PPC displayed inversely from 87° to 98°. Both of the two LC compounds consisted of stiff backbones and flexible side-chains, the stiff backbones tended to orderly orientate while the soft side chains tended to randomly arrange. For PU/PPC system, the side chains of PPC were shorter and consequently less entangled with the soft segments of PU. Therefore, in the formation of PU/PPC membrane, when the stiff backbones began to arrange in order, the soft side-chains kept moving until the solvent was completely evaporated, such that the hydrophobic aliphatic side-chains tended to distribute on the surface of the composite membranes that made the PU/PPC exhibited gradually hydrophobic with the enhancement of PPC content. Conversely, for PU/OPC complexes, the flexible side-chains of OPC were longer and entangled with the soft segments of PU with a relative higher degree, which resulted in a greater influence on the arrangement of the stiff backbones. The OPC backbones with more hydrophilic groups were unable to preferentially assemble in order during the formation of membranes, but mainly aggregated on the membrane surface so that the hydrophilicity of composite membranes increased with the increase of LC content.

These results indicated that LC alignment behaviors were closely related to the alkyl side-chain length, and consequently played a distinct influential role on surface morphology and properties of composite membranes.

3.5. Cell compatibility of PU/LC composite membranes

3.5.1. Cell viability test

The viability of 3T3 fibroblast cultured on the two PU/LC composite membranes with various LC ratios was evaluated over different periods (1, 3, 5 and 7 days) by MTT assay, as shown in Fig. 7. Although the cells growth was similar for both membranes after 1 day culture, the proliferation rate of cells got different gradually from each other with the culture time. At the same culture period, cells presented higher viability on PU/LC composite membrane with the increase of LC content. For the PU/PPC composite, only at a PPC proportion of over 50%, cells showed comparable viability as that on controlled pure PU films. Nevertheless, all the PU/OPC composite membranes showed a better viability than the pure PU matrix. It seemed that the LC type have an effect on the cell viability of the PU/LC composite. It was possible that the longer flexible side chains of OPC weakened the rigidity of the backbone and made the molecular much softer (Rey, 2005), thus the rich-OPC domains on the composite surface presented better fluidity that might be potentially beneficial for cells proliferation (Lockwood et al., 2006).

3.5.2. Cell initial adhesion and morphology

The cell behaviors, such as cell adhesion, spreading, proliferation and differentiation on material surfaces are the key factors for the evaluation of cytocompatibility of a novel biomaterial (Bettini et al., 2008). The cell initial adhesion after 2 h of incubation was shown in Fig. 8a–e. Fibroblasts adhered on the surface of pure PU film (Fig. 8a) by means of thin cytoplasmic digitations, and began to change their morphology from round to elongated shape. On the PU/OPC composite membranes (Fig. 8b–e), fibroblasts gradually presented better attachment with the increase of OPC content. When the proportion of OPC was less than 50% (Fig. 8b and c), cells remained oval shape and exhibited rare digitation or filament, indicating that the cell-surface contact was not enough stable and the cells were still probing for appropriate adhesion sites (Schulte et al., 2010). When the OPC content reached over 50% (Fig. 8d and e) cells displayed favorable attachment and generated filopodia-like extension. Comparing with PU/OPC composite film, PU/PPC complex presented lower affinity with cells, and the fibroblast initially adhered on the membranes in a spherical shape (data not shown). It indicated that the PU/OPC composite membrane was more in favor of the initial adhesion of cells at the same LC content.

After 3 days of incubation, the morphologies of fibroblasts on the PU/OPC composite membranes were shown in Fig. 8f–j. At a LC ratio of less than 30%, fibroblasts were individually spread and some of them still maintained oval morphology on membranes (Fig. 8g and h), which was similar to those on the controlled pure PU film (Fig. 8f). However, cells were in high density, largely confluent, formed a cellular unity and exhibited a flat morphology on membranes with a LC content of more than 50% (Fig. 8i and j). It suggested that a higher cells density was obtained on the membrane with a larger proportion of LC, which was consistent with the result of the MTT test. Superior spread and proliferation of cells was observed on PU/OPC complex in comparison to PU/PPC composite membrane at the same content of LC (data not shown).

Previous researches have demonstrated that biomembrane is predominantly lipid bilayer showing liquid crystal phase with the essential features of fluidity and diffusion (Zeng & Li, 2011). It was reported that liquid crystalline polymers could be compatible with cells in living systems (Nagahama et al., 2007) for the self-organizing structures of liquid crystals by noncovalent specific interactions. In this study, LC domains, embedding into PU matrix, endowed the membrane surface with the feature of fluidity, which might be similar to the hyperelastic extracellular matrix (Zeng & Li, 2011). This kind of elastic fluids in liquid crystal state made them potentially favorable for cells growth and proliferation. In the PU/LC composite, rich-OPC domains would be more elastic in comparison to rich-PPC regions due to the longer flexible branches of OPC molecules, and consequently facilitated cell adhesion (Ryser, 1967; Singh, Kasinath, & Lewis, 1992; Woltman et al., 2007).

When LC was at low concentration, the LC formed discrete small size island-like droplets dispersing throughout the composite membrane surfaces. With the increment of LC content, more rich-LC domains were generated and gradually coalesce with each other (as shown in Fig. 3), such that the fluidity of composite membrane surface increased. Therefore, the improved molecular mobility, which was similar to the movable morphology of the nature biomembrane surface, made these membranes exhibit favorable cytocompatability (Hwang et al., 2002). Compared with PU/PPC membrane, PU/OPC membrane showed a better cell compatibility maybe attributed to its lower crystallinity and higher hydrophilicity (Padial-Molina et al., 2011). These results indicated that the concentration and type of LC could have an influence on the surface morphology and cytocompatibility of membrane.

4. Summary

Two types of PU/LC composite membranes were studied in this paper. All PU/LC composite membranes showed the similar coarse surfaces and two-phase morphology. The introduction of LC into PU matrix disrupted the crystallization of PU. Due to the different length of flexible side-chains, PPC tended to aggregate to form independent phase which resulted in the formation of larger LC domains, while the OPC organized uniform distribution among the composite. The significant different arrangement of OPC and PPC in the complex led to the reversal tendency of water contact angle of the composite membranes with the increase of LC content. The cultivation of 3T3 fibroblast on the PU/LC composite

membranes showed different cells adhesion, spread and proliferation with different contents and types of LC. Cells presented poor attachment and proliferation with a LC content of lower than 30%, and exhibited good growth and filopodia-like extension when LC content was over 30%. The PU/OPC composite membranes presented better cytocompatibility than the PU/PPC complex at the same LC ratio. The results demonstrated that the surface properties of PU/LC composite membrane, including size, distribution, texture and arrangement of LC domains, the phase separation as well as the wettability had significant effects on the cell behaviors. The PU/LC composite membrane with excellent cytocompatibility may be a potential candidate for cells growth.

Acknowledgements

This work was supported by National Nature Science Foundation of China (31170911, 30870613 and 31040027), Scientific Research Cultivation and Innovation Funds of Jinan University (21610607), Special Funds for Base Construction of Industry, Education and Research of Guangdong Province (2009GJE00008) and Project for the scientists and technicians serving enterprises in Guangdong (2009GJE00008).

References

Aouada, F. A., De Moura, M. R., Fernandes, P. R. G., Rubira, A. F., & Muniz, E. C. (2005). Optical and morphological characterization of polyacrylamide hydrogel and liquid crystal systems. *European Polymer Journal*, *41*, 2134–2141.

Bettini, R., Romani, A. A., Morganti, M. M., & Borghetti, A. F. (2008). Physicochemical and cell adhesion properties of chitosan films prepared from sugar and phosphate-containing solutions. *European Journal of Pharmaceutics and Biopharmaceutics*, *68*, 74–81.

Bouligand, Y., & Norris, V. (2001). Chromosome separation and segregation in dinoflagellates and bacteria may depend on liquid crystalline states. *Biochimie*, *83*, 187–192.

Bruckmann, C., Walboomers, X. F., Matsuzaka, K., & Jansen, J. A. (2005). Periodontal ligament and gingival fibroblast adhesion to dentin-like textured surfaces. *Biomaterials*, *26*, 339–346.

Caffrey, M. (2003). Membrane protein crystallization. *Journal of Structural Biology*, *142*, 108–132.

De Oca, H. M., Wilson, J. E., Penrose, A., Langton, D. M., Dagger, A. C., Anderson, M., et al. (2010). Liquid-crystalline aromaticealiphatic copolyester bioresorbable polymers. *Biomaterials*, *31*, 7599–7605.

Fong, W. K., Hanley, T., & Boyd, B. J. (2009). Stimuli responsive liquid crystals provide 'on-demand' drug delivery in vitro and in vivo. *Journal of Controlled Release*, *135*, 218–226.

Gong, L. (2011). *Study on the synthesis of hydroxypropyl cellulose esters liquid crystals and the cell compatibility of their polymer-based composite membranes*. Master's Thesis. Jinan University.

Hwang, J. J., Iyer, S. N., Li, L. S., Claussen, R., Harrington, D. A., & Stupp, S. I. (2002). Self-assembling biomaterials: Liquid crystal phases of cholesteryl oligo(L-lactic acid) and their interactions with cells. *PNAS*, *99*, 9662–9667.

Ignés-mullol, J., & Schwartz, A. K. (2001). Shear-induced molecular precession in a hexatic Langmuir monolayer. *Nature*, *410*, 348–351.

Kaneko, T., Yamaoka, K., Osada, Y., & Gong, J. P. (2004). Thermoresponsive shrinkage triggered by mesophase transition in liquid crystalline physical hydrogels. *Macromolecules*, *37*, 5385–5388.

Kasemo, B. (2002). Biological surface science. *Surface Science*, *500*, 656–677.

Kovacevic, V., Kljajie-Malinovic, L. J., Smit, I., Bravar, M., Agic, A., & Cerovecki, Z. (1990). Adhesive composition systems in degradative conditions. In K. W. Allen (Ed.), *Adhesion 14* (pp. 126–160). London: Elsevier Applied Science.

Kovacevic, V., Smit, I., Hace, D., Suceska, M., Mundri, I., & Bravar, M. (1993). Role of the polyurethane component in the adhesive composition on the hydrolytic stability of the adhesive. *International Journal of Adhesion and Adhesives*, *13*, 126–136.

Li, L. H., Tu, M., Mou, S. S., & Zhou, C. R. (2001). Preparation and blood compatibility of polysiloxane/liquid-crystal composite membranes. *Biomaterials*, *22*, 2595–2599.

Lin, H. K., Huang, Y. F., & Chen, A. C. (2011). Texture evolution of cholesteric liquid crystal driven by a thermal process. *Applied Surface Science*, *257*, 9858–9862.

Lockwood, N. A., Mohr, J. C., Ji, L., Murphy, C. J., Palecek, S. P., De Pablo, J. J., et al. (2006). Thermotropic liquid crystals as substrates for imaging the reorganization of matrigel by human embryonic stem cells. *Advanced Functional Materials*, *16*, 618–624.

Lutolf, M. P., Gilbert, P. M., & Blau, H. M. (2009). Designing materials to direct stem-cell fate. *Nature*, *462*, 433–441.

Ma, Z. W., Mao, Z. W., & Gao, C. Y. (2007). Surface modification and property analysis of biomedical polymers used for tissue engineering. *Colloids and Surfaces B: Biointerfaces*, *60*, 137–157.

Matsusaki, M., Thi, T. H., Kaneko, T., & Akashi, M. (2005). Enhanced effects of lithocholic acid incorporation into liquid-crystalline biopolymer poly(coumaric acid) on structural ordering and cell adhesion. *Biomaterials*, *26*, 6263–6270.

Nagahama, K., Ueda, Y., Ouchi, T., & Ohya, Y. (2007). Exhibition of soft and tenacious characteristics based on liquid crystal formation by introduction of cholesterol groups on biodegradable lactide copolymer. *Biomacromoleclules*, *8*, 3938–3943.

Padial-Molina, M., Galindo-Moreno, P., Fernández-Barbero, J. E., O'Valle, F., Jódar-Reyes, A. B., Ortega-Vinuesa, J. L., et al. (2011). Role of wettability and nanoroughness on interactions between osteoblast and modified silicon surfaces. *Acta Biometerialia*, *7*, 771–778.

Ranella, A., Barberoglou, M., Bakogianni, S., Fotakis, C., & Stratakis, E. (2010). Turning cell adhesion by controlling the roughness and wettability of 3D micro/nano silicon structures. *Acta Biomaterialia*, *6*, 2711–2720.

Rey, A. D. (2005). Mechanics of soft-solid–liquid-crystal interfaces. *Physical Review E*, *72*, 1–15.

Ryser, H. J. P. (1967). A membrane effect of basic polymers dependent on molecular size. *Nature*, *215*, 45–46.

Schulte, V. A., Hu, Y., Diez, M., Bünger, D., Möller, M., & Lensen, M. C. (2010). A hydrophobic perfluoropolyether elastomer as a patternable biomaterial for cell culture and tissue engineering. *Biomaterials*, *31*, 8583–8595.

Singh, A. K., Kasinath, B. S., & Lewis, E. J. (1992). Interaction of polycations with cell-surface negative charges of epithelial cells. *Biochimica et Biophysica Acta*, *1120*, 337–342.

Singhvi, R., Stephanopoulos, G., & Wang, D. I. C. (1994). Effects of substratum morphology on cell physiology. *Biotechnology and Bioengineering*, *43*, 764–771.

Smeller, L. (2002). Pressure–temperature phase diagrams of biomolecules. *Biochimica et Biophysica Acta (BBA): Protein Structure and Molecular Enzymology*, *1595*, 11–29.

Stewart, G. T. (2003). Liquid crystals in biology. I. Historical, biological and medical aspects. *Liquid Crystals*, *30*, 541–557.

Stewart, G. T. (2004). Liquid crystals in biology. II. Origins and processes of life. *Liquid Crystals*, *31*, 443–471.

Vihola, H., Laukkanen, A., Valtola, L., Tenhu, H., & Hirvonen, J. (2005). Cytotoxicity of thermosensitive polymers poly(N-isopropylacrylamide), poly(N-vinylcaprolactam) and amphiphilically modified poly(N-vinylcaprolactam). *Biomaterials*, *26*, 3055–3064.

Woltman, S. J., Jay, G. D., & Crawford, G. P. (2007). Liquid-crystal materials find a new order in biomedical applications. *Nature Materials*, *6*, 929–938.

Xie, Q. Y. (2007). *The preparation and biology of polyurethane/cellulose derivative liquid crystal compound membrane*. Master's Thesis. Jinan University.

Zeng, X., & Li, S. (2011). Multiscale modeling and simulation of soft adhesion and contact of stem cells. *Journal of the Mechanical Behavior of Biomedical Materials*, *4*, 180–189.

Zhou, C. R., & Yi, Z. J. (1999). Blood-compatibility of polyurethane/liquid crystal composite membranes. *Biomaterials*, *20*, 2093–2099.